Articles

Water-Assisted H−H Bond Splitting Mediated by [CpRu(PTA)$_2$Cl] (PTA=1,3,5-triaza-7-phosphaadamantane). A DFT Analysis

Andrea Rossin,[†] Luca Gonsalvi,[†] Andrew D. Phillips,[†] Olivier Maresca,[‡] Agustí Lledós,*[,‡] and Maurizio Peruzzini*[,†]

Consiglio Nazionale delle Ricerche, Istituto di Chimica dei Composti Organometallici (ICCOM-CNR), Via Madonna del Piano 10, 50019 Sesto Fiorentino (Firenze), Italy, and Departament de Química, Universitat Autònoma de Barcelona, Bellaterra, Barcelona, Spain

Received November 7, 2006

A DFT study using a "discrete-continuum" modeling of the reaction medium, employed to unravel the role of water in the activation of dihydrogen by [CpRu(PTA)$_2$Cl] (PTA = 1,3,5-triaza-7-phosphaadamantane), has revealed that the solvent takes an active part in lowering the energy barriers of the overall heterolytic splitting of the H−H bond. PTA itself promotes the heterolytic activation of the Ru(η^2-H$_2$) bond through one of its nitrogen atoms via a solvent-mediated intramolecular proton transfer.

Introduction

The importance of metal-promoted hydrogen activation has been recognized for at least four decades,[1] and much attention has been dedicated since then to the various aspects of this field, including catalyst design and testing, mechanistic investigations and theoretical calculations of the reaction pathways, and the nature of transition states and intermediates involved.[2]

A common feature of many catalytic hydrogenation systems is the presence of active species containing one or more hydrogen atoms coordinated in different forms to the metal. These may include either nonclassical dihydrogen ligands and classical dihydrides or monohydrides, the latter generated primarily via base-assisted intra- or intermolecular heterolytic dihydrogen splitting.[3] Comprehensive reviews and relevant articles on H$_2$ activation have recently appeared in the literature,[2−4] including a recent account of H−H heterolytic splitting.[5] However, a clear and complete picture of H$_2$ heterolysis in different solvent systems, especially in polar ones like water, has not been attained as yet.

We have been interested for some years in catalytic reduction of various organic substrates in biphasic systems using water-soluble Ru(II) complexes such as [CpRu(PTA)$_2$Cl] (**1**) (Cp = C_5H_5; PTA = 1,3,5-triaza-7-phosphaadamantane).[6] HPNMR measurements carried out under high H$_2$ pressure (30 bar) and temperature (45−80 °C) in an *n*-octane/water biphasic system mimicking the catalytic reaction conditions indicated that the *mono*hydrido complex [CpRu(PTA)$_2$H] (**2**) is formed under these conditions.[7] Later reports by Frost et al. showed elegantly the pH-dependent speciation of aqueous solutions of **2** under a pressure of hydrogen, where it emerged that one or both PTA ligands can be protonated at one nitrogen atom, yielding complexes [CpRu(PTA){PTA(H)}H]$^+$ (**3**) and [CpRu{PTA-(H)}$_2$H]$^{2+}$ (**4**) as observed by NMR (Scheme 1).[8]

Complex **3** was proposed as the active catalytic species for benzylidene acetone reduction by the authors. The study was complemented by DFT calculations of the relative energies of the various protonated species of [CpRu(PTA)$_2$H] in the gas phase, which however cannot account for the interaction of such species with a noninnocent solvent such as water. On the basis of the experimental findings outlined above, we decided to investigate the effect of the solvent on the reaction mechanism underlying the H−H bond activation through the metal in water. Herein, a DFT computational study of the H−H splitting in water mediated by [CpRu(PTA)$_2$Cl] is presented. Both the

* Corresponding author. E-mail: agusti@klingon.uab.es (A.L.); mperuzzini@iccom.cnr.it (M.P.).

† Istituto di Chimica dei Composti Organometallici.

‡ Universitat Autònoma de Barcelona.

(1) Historically important papers on molecular hydrogen activation include: (a) Halpern, J. *J. Phys. Chem.* **1959**, *63*, 398. (b) Kubas, G. J.; Ryan, R. R.; Swanson, B. I.; Vergamini, P. J.; Wasserman, H. J. *J. Am. Chem. Soc.* **1984**, *106*, 451. (c) Lee, J. C., Jr.; Rheingold, A. L.; Muller, B.; Pregosin, P. S.; Crabtree, R. H. *J. Chem. Soc., Chem. Commun*. **1994**, 1021. (d) Morris, R. H.; Schlaf, M. *Inorg. Chem.* **1994**, *33*, 1725.

(2) See for example: (a) James, B. R. *Homogeneous Hydrogenation*; Wiley: New York, 1973. (b) Jessop, G.; Morris, R. H. *Coord. Chem. Rev.* **1992**, *121*, 155. (c) Heinekey, D. M.; Oldham, W. J., Jr. *Chem. Rev.* **1993**, *93*, 913. (d) Crabtree, R. H. *Angew. Chem., Int. Ed. Engl.* **1993**, *32*, 789. (e) Stanislaus, A.; Cooper, B. H. *Catal. Rev.* **1994**, *36*, 75. (f) Morris, R. H. *Can. J. Chem.* **1996**, *74*, 1907. (g) Torrent, M.; Solà, M.; Frenking, G. *Chem. Rev.* **2000**, *100*, 439. (h) Heinekey, D. M.; Lledós, A.; Lluch, J. M. *Chem. Soc. Rev.* **2004**, *33*, 175. (i) *The Handbook of Homogeneous Hydrogenation*; de Vries, J. G., Elsevier, C. J., Eds.; Wiley-VCH: Weinheim, D, 2006.

(3) For recent books on this topic, see: (a) *Recent Advances in Hydride Chemistry*; Peruzzini, M., Poli, R., Eds.; Elsevier SA: Amsterdam, NL, 2001. (b) *Metal Dihydrogen and σ-bond Complexes*; Kubas, G. J., Ed.; Kluwer/Academic Plenum Publishers: New York, 2001.

(4) (a) Maseras, F.; Lledós, A.; Clot, E.; Eisenstein, O. *Chem. Rev.* **2000**, *100*, 601. (b) Niu, S.; Hall, M. B. *Chem. Rev.* **2000**, *100*, 353. (c) Ienco, A.; Calhorda, M. J.; Reinhold, J.; Reineri, F.; Bianchini, C.; Peruzzini, M.; Vizza, F.; Mealli, C. *J. Am. Chem. Soc.* **2004**, *126*, 11954.

(5) Kubas, G. J. *Adv. Inorg. Chem.* **2004**, *56*, 127.

(6) Bolaño, S.; Gonsalvi, L.; Zanobini, F.; Vizza, F.; Bertolasi, V.; Romerosa, A.; Peruzzini, M. *J. Mol. Catal. A: Chem*. **2004**, *224*, 61.

(7) Akbayeva, D. N.; Gonsalvi, L.; Oberhauser, W.; Peruzzini, M.; Vizza, F.; Brüggeller, P.; Romerosa, A.; Sava, G.; Bergamo, A. *Chem. Commun.* **2003**, 264.

(8) (a) Frost, B. J.; Mebi, C. A. *Organometallics* **2004**, *23*, 5317. (b) Mebi, C. A.; Frost, B. J. *Organometallics* **2005**, *24*, 2339. (c) Mebi, C. A.; Nair, R. P.; Frost, B. J. *Organometallics* **2007**, *26*, 429.

10.1021/om061023a CCC: $37.00
Publication on Web 05/26/2007

Scheme 1. Schematic Drawings of Complexes 1−4

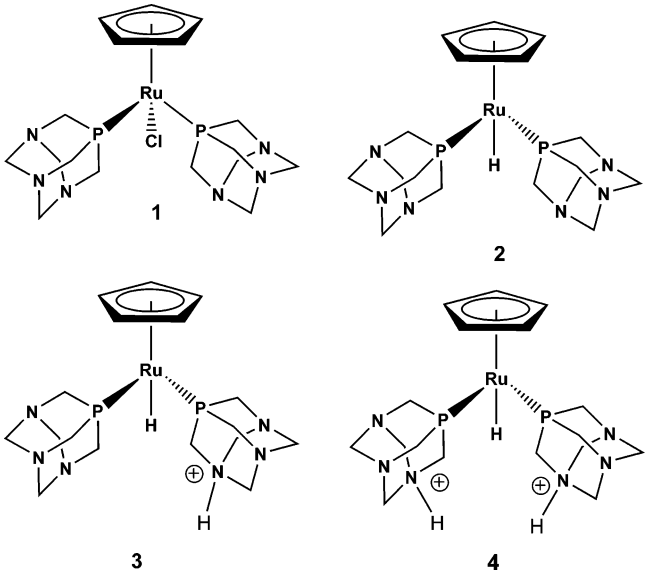

homolytic (oxidative addition) and the heterolytic pathways have been investigated, and a rationale for the nature of the hydrides observed experimentally is proposed.

Computational Details

All the calculations were performed with the Gaussian03 software package[9] at the DFT/B3LYP level.[10] A crucial feature of the present work is the analysis of the solvent intervention in the H−H bond breaking process. For this purpose a discrete-continuum modeling of the reaction medium was employed, including solvent effects both by the polarizable continuum model (PCM)[11] and by the explicit introduction in the computational system of discrete water molecules. The "discrete aqueous medium" consists of a cluster of three neutral molecules $(H_2O)_3$, interbound by hydrogen bonds. A single water molecule is not enough to give a realistic description of the medium, since proton exchange processes that take place during the reaction imply transfer of charges with formation of highly reactive ions. The choice of three water molecules to reproduce the reaction medium in aqueous-biphasic systems was proven to be the best compromise between a realistic description and system size, in earlier investigations by Kovács et al., to model theoretically the $[Ru(TPPMS)_xH_2]$-catalyzed hydrogenation of cinnamaldehyde in water ($x = 3, 4$; TPPMS = *meta*-sulfonatophenyldiphenylphosphine).[12]

The optimization of minima and transition states was carried out using the water-cluster model. Frequency calculations were performed on all the optimized structures, to characterize the stationary points as minima or TSs, as well for the calculation of zero-point energies, enthalpies, entropies, and gas-phase Gibbs energies at 298 K. IRC analysis[13] was performed, to find the two minima linked by the related transition structure. When IRC calculations failed to reach the minima, geometry optimizations from the initial phase of the IRC path were performed. For all the optimized structures, the effect of the bulk aqueous medium ($\epsilon = 78.4$) was then estimated by the application of PCM single-point calculations using standard UA0 solvation spheres. Individual solvation cavities were added on the H atoms bonded to ruthenium and also on all the H atoms of the water chain $(H_2O)_3$. The Gibbs energies in water (ΔG_{water}) were obtained, adding to the Gibbs energies in the gas phase the contribution of the Gibbs energy of solvation from the continuum model.

Optimizations and characterization of the stationary points were performed with basis set 1 (BS1). In this basis set core electrons of the Ru, Cl, and P atoms were described using the pseudopotentials of Hay and Wadt,[14] and their valence electrons were expressed through a LANL2DZ basis set.[9] In the case of the Cl and P atoms, an extra d-type polarization function was added to the standard basis set.[15] The C atoms of the Cp ligand were described with a 6-31G(d) basis set, the hydridic H atoms were described with a 6-31G(d,p) basis set, and finally all the remaining C and H atoms, together with the O atoms of the water molecules (where present), were described with a 6-31G basis.[16] An extended hydrogen-bonded network involving the three water molecules and the basic centers of the complexes was found in all the optimized structures. To better estimate the energies of such structures, the energies of all the minima and transition sates were recalculated using an extended basis set (BS2) with single-point calculations at the geometries optimized with BS1. In basis set 2 polarization functions are added to all the atoms, including the water molecules: p for all the hydrogens (6-31G(d,p)), d for the O atoms of the water molecules and the N atoms of PTA ligands (6-31G(d)), and f for the metal.[16,17]

Results and Discussion

1. Dihydrogen Complex Formation from the Chloride Precursor. As it was observed experimentally by some of us[7] and others,[8b] in order to obtain a catalytically active species from $[CpRu(PTA)_2Cl]$, the initial step must consist of the heterolytic Ru−Cl bond cleavage, yielding the unsaturated $[CpRu(PTA)_2]^+$ fragment and releasing the Cl^- anion, a process favored in water. The rather low energy value for this bond-breaking process in water (29.1 kcal/mol) is a consequence of

(9) Frisch, M. J.; Trucks, G. W.; Schlegel, H. B.; Scuseria, G. E.; Robb, M. A.; Cheeseman, J. R.; Montgomery, J. A., Jr.; Vreven, T.; Kudin, K. N.; Burant, J. C.; Millam, J. M.; Lyengar, S. S.; Tomasi, J.; Barone, V.; Mennucci, B.; Cossi, M.; Scalmani, G.; Rega, N.; Petersson, G. A.; Nakatsuji, H.; Hada, M.; Ehara, M.; Toyota, K.; Fukuda, R.; Hasegawa, J.; Ishida, M.; Nakajima, T.; Honda, Y.; Kitao, O.; Nakai, H.; Klene, M.; Li, X.; Knox, J. E.; Hratchian, H. P.; Cross, J. B.; Adamo, C.; Jaramillo, J.; Gomperts, R.; Stratmann, R. E.; Yazyev, O.; Austin, A. J.; Camml, R.; Pomelli, C.; Ochterski, J. W.; Ayala, P. Y.; Morokuma, K.; Voth, G. A.; Salvador, P.; Dannenberg, J. J.; Zakrzewski, V. G.; Dapprich, S.; Daniels, A. D.; Strain, M. C.; Farkas, O.; Malick, D. K.: Rabuck, A. D.; Raghavachari, K.; Foresman, J. B.; Ortiz, J. V.; Cui, Q.; Baboul, A. G.; Clifford, S.; Cioslowski, J.; Stefanov, B. B.; Liu, G.; Liashenko, A.; Piskorz, P.; Komaromi, I.; Martin, R. L.; Fox, D. J.; Keith, T.; Al-Laham, M. A.; Peng, C. Y.; Nanayakkara, A.; Challacombe, M.; Gill, P. M. W.; Johnson, B.; Chen, W.; Wong, M. W.; Gonzalez, C.; Pople, J. A. *Gaussian 03*, revision C.02; Gaussian, Inc.: Pittsburgh, PA, 2004.

(10) (a) Lee, C.; Parr, R. G.; Yang, W. *Phys. Rev. B* **1988**, *37*, 785. (b) Becke, A. D. *J. Chem. Phys.* **1993**, *98*, 5648. (b) Stephens, P. J.; Devlin, J. F.; Chabalowski, C. F.; Frisch, M. J. *J. Phys. Chem.* **1994**, *98*, 11623.

(11) Cossi, M.; Barone, V.; Cammi, R.; Tomasi, J. *Chem. Phys. Lett.* **1996**, *255*, 327.

(12) (a) Kovacs, G.; Schubert, G.; Joó, F.; Papai, I. *Organometallics* **2005**, *24*, 3059. (b) Kovács, G.; Ujaque, G.; Lledós, A.; Joó, F. *Organometallics* **2006**, *25*, 862. (c) Rossin, A.; Kovács, G.; Ujaque, G.; Lledós, A.; Joó, F. *Organometallics* **2006**, *25*, 5010.

(13) Fukui, K. *Acc. Chem. Res.* **1981**, *14*, 363.

(14) (a) Hay, P. J.; Wadt, W. R. *J. Chem. Phys.* **1985**, *82*, 270. (b) Wadt, W. R.; Hay, P. J. *J. Chem. Phys.* **1985**, *82*, 284.

(15) Höllwarth, A.; Böhme, M.; Dapprich, S.; Ehlers, A. W.; Gobbi, A.; Jonas, V.; Köhler, K. F.; Stegmann, R.; Veldkamp, A.; Frenking, G. *Chem. Phys. Lett.* **1993**, *208*, 237.

(16) (a) Hehre, W. J.; Ditchfield, R.; Pople, J. A. *J. Chem. Phys.* **1972**, *56*, 2257. (b) Hariharan, P. C.; Pople, J. A. *Theor. Chim. Acta* **1973**, *28*, 213. (c) Francl, M. M.; Pietro, W. J.; Hehre, W. J.; Binkley, J. S.; DeFrees, D. J.; Pople, J. A.; Gordon, M. S. *J. Chem. Phys.* **1982**, *77*, 3654.

(17) Ehlers, A. W.; Böhme, S.; Dapprich, S.; Gobbi, A.; Höllwarth, A.; Jonas, V.; Köhler, K. F.; Stegmann, R.; Veldkamp. A.; Frenking, G. *Chem. Phys. Lett.* **1993**, *208*, 111.

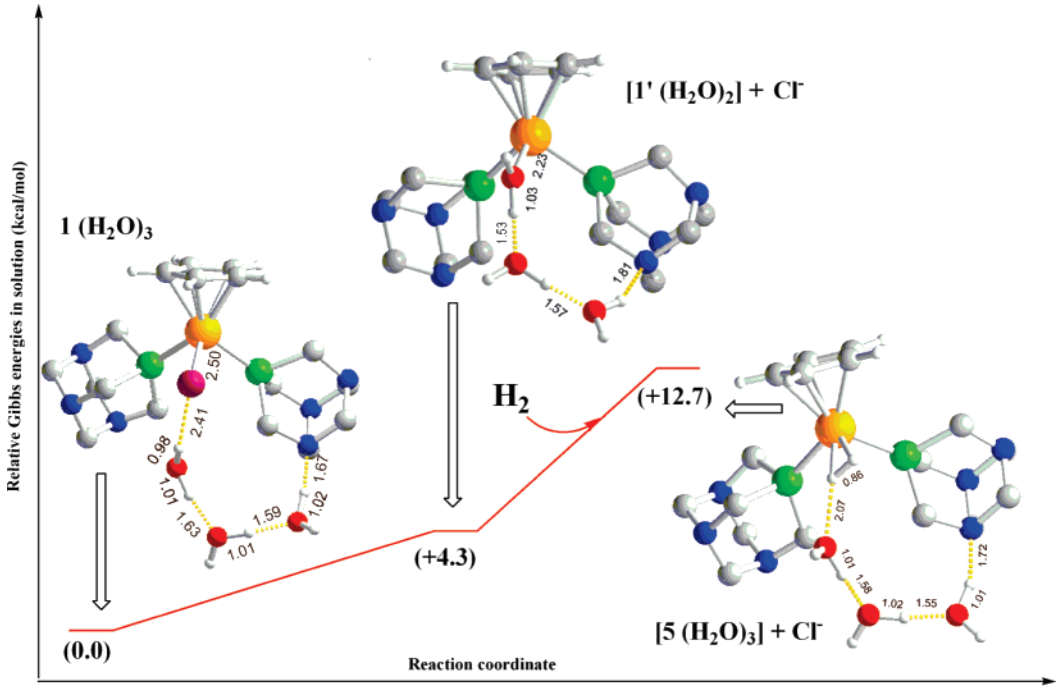

Figure 1. Gibbs energy profile in water for the chloride by H_2 ligand exchange, starting from {**1·(H$_2$O)$_3$**} and leading to the formation of the dihydrogen complex {[CpRu(PTA)$_2$(η^2-H$_2$)]$^+$·(H$_2$O)$_3$} {**5·(H$_2$O)$_3$**}. Atom color code: orange, ruthenium; light gray, carbon; white, hydrogen; green, phosphorus; purple, chlorine; blue, nitrogen. Hydrogen atoms on the PTA ligands were omitted for clarity. Hydrogen bonds are depicted in yellow. Bond distances are in angstroms.

the high solvation Gibbs energy of the chloride anion in this solvent ($\Delta G_{solv}(Cl^-) = -78.5$ kcal/mol).[18]

Starting from **1**, the water adduct {**1·(H$_2$O)$_3$**} was optimized first, and displacement of the chloride by H_2 was then examined (Figure 1). It is interesting to point out that after checking several possibilities we found that the lowest minimum for {**1·(H$_2$O)$_3$**} corresponds to an arrangement of the three water molecules making a hydrogen-bonded chain that connects two basic centers of the molecule (the chloride and a nitrogen atom from one PTA ligand). As we will show later, we have found the same water molecule configuration in all the structures.

Then we considered the unsaturated species [CpRu(PTA)$_2$]$^+$ resulting from the Cl^- dissociation. However, the optimization of this unsaturated species in the presence of three water molecules results in the coordination of one water molecule to the metal (Ru−O$_w$ = 2.235 Å), giving the aquo complex {[CpRu(PTA)$_2$(H$_2$O)]$^+$·(H$_2$O)$_2$}, {**1′·(H$_2$O)$_2$**}. In this complex one water molecule occupies the empty coordination site on ruthenium, while the other two water molecules connect by a hydrogen-bonding network a proton of the water ligand with a nitrogen atom of one PTA ligand. The presence of water strongly favors chloride dissociation and subsequent formation of the aquo complex {[CpRu(PTA)$_2$(H$_2$O)]$^+$·(H$_2$O)$_2$}, more stable than its isolated components [CpRu(PTA)$_2$]$^+$ and (H$_2$O)$_3$ (ΔG_{water} = 14.8 kcal/mol). The stability of the monoaquo complex [CpRu(PTA)$_2$(H$_2$O)]$^+$ agrees with its experimental NMR detection by dissolving **1** in water.[19] Displacement of the coordinated water by H_2, resulting in the complex {[CpRu(PTA)$_2$(η^2-H$_2$)]$^+$·(H$_2$O)$_3$}, {**5·(H$_2$O)$_3$**}, is endoergonic. The dihydrogen complex [CpRu(PTA)$_2$(η^2-H$_2$)]$^+$ has not been observed.[7,8a] However the formation of this key initial intermediate from which the H−H activation starts can be driven by the high H_2 presssures at which the reaction is being performed,[7,8] even if it is reasonable that, under these conditions, it rapidly evolves to more stable species. The dihydrogen complex **5** showed a calculated H−H bond length of 0.862 Å, slightly longer than that of free H_2 (0.78 Å), as a consequence of the simultaneous $\sigma_{(H-H)} \rightarrow$ empty $d_{(Ru)}$ donation and filled $d_{(Ru)} \rightarrow \sigma^*_{(H-H)}$ back-donation.[2−4] The presence of a hydrogen bond between the acidic dihydrogen ligand and the oxygen of the closest water molecule can be inferred from the O−H$_{dihydrogen}$ distance (2.067 Å), and it also contributes to the H−H lengthening. The dihydrogen ligand is not symmetrically coordinated to the metal. The Ru−H distance for the H atom participating in the hydrogen bond (1.793 Å) is significantly elongated with respect to the other one (1.714 Å). In this way {**5·(H$_2$O)$_3$**} can be considered an incipient stage of the heterolytic activation. Very recently, experimental evidence that the coordinated H_2 ligand can participate in intermolecular hydrogen bonding to H-bond acceptors has been given.[20]

Overall the first step of the reaction leads to the substitution of an anionic Cl^- ligand by the weaker neutral H_2 ligand. Our study has proved that despite the different intrinsic binding energies of both ligands in water, this process can be possible as a consequence of both the high ΔG_{solv} of the released chloride anion by the bulk solvent and the specific hydrogen-bonding interactions with discrete water molecules.

2. H−H Bond Breaking: Homolytic versus Heterolytic Pathway. The H−H bond in {**5·(H$_2$O)$_3$**} can be activated in principle following either a homolytic or a heterolytic pathway. The homolytic splitting does not require any direct solvent participation to occur, and it can be seen as a formal oxidative addition of the H−H bond to Ru(II) affording a Ru(IV) dihydride. To date, there are no reports of *cis*-dihydride complexes [CpRu(PR$_3$)$_2$H$_2$]$^+$ either isolated or spectroscopically detected. Likewise we were unable to locate a minimum

(18) This value is in very good agreement with accurate evaluations of the chloride solvation Gibbs energy recently reported: Kelly, C. P.; Cramer C. J.; Truhlar, D. G. *J. Phys. Chem. B* **2006**, *110*, 16066.

(19) Lidrissi, C.; Romerosa, A.; Saoud, M.; Serrano-Ruiz, M.; Gonsalvi, L.; Peruzzini, M. *Angew. Chem., Int. Ed.* **2005**, *44*, 2568.

(20) Szymczak, N. K.; Zakharov, L. N.; Tyler, D. R. *J. Am. Chem. Soc.* **2006**, *128*, 15830.

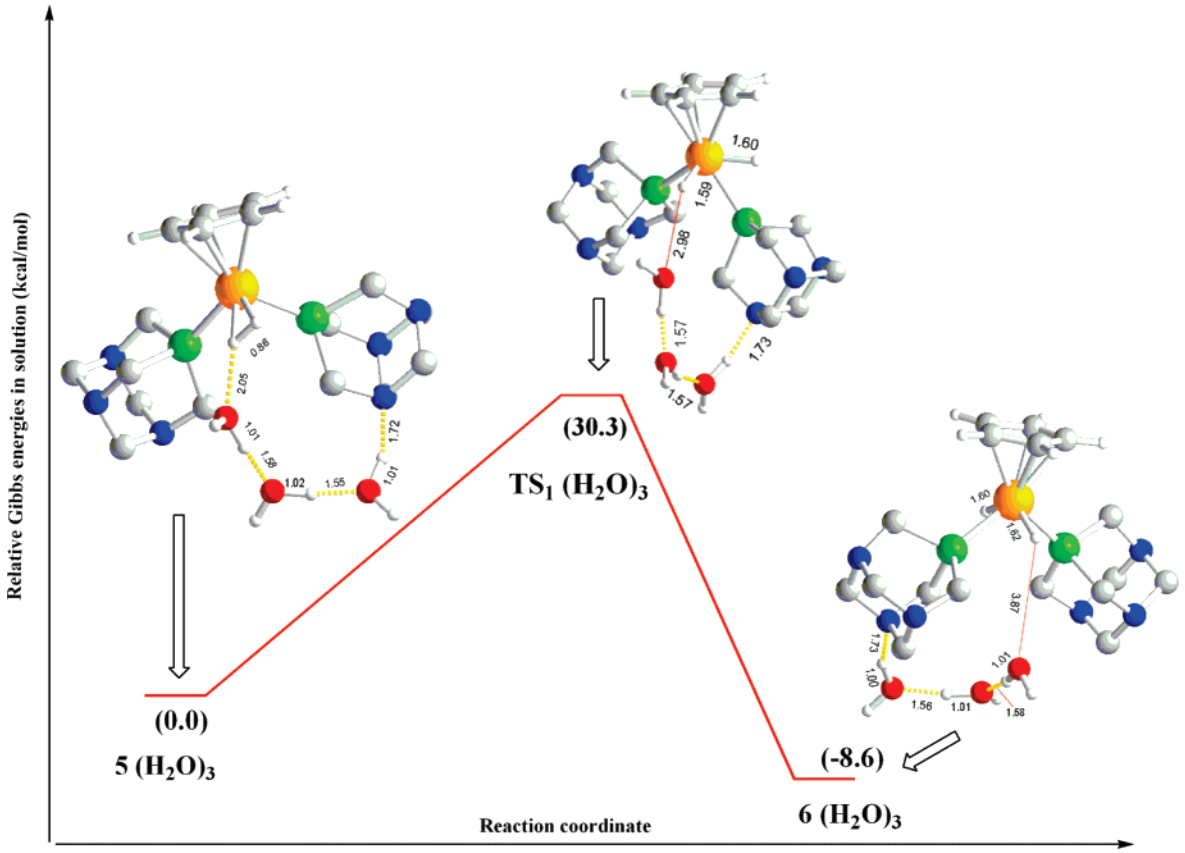

Figure 2. Gibbs energy profile in water for the dihydrogen → dihydride isomerization through the homolytic pathway. Hydrogen atoms of the PTA ligands were omitted for clarity. For atom colors, refer to the caption in Figure 1. Selected bond lengths are reported in angstroms.

corresponding to a *cis*-dihydride species. That implies that, as for other group 8 half-sandwich $[CpM(PR_3)_2H_2]^+$ (M = Fe,[21] Ru[22]), the dihydrogen → dihydride interconversion is an important stereochemical change, passing from the three-legged piano-stool dihydrogen complex to a *transoid* square-based four-legged piano-stool dihydride. Thus, the homolytic cleavage of the H−H bond should be accompanied by a *cis*−*trans* rearrangement, which involves the migration of one H atom from one side of the molecule to the opposite side. The resulting complex would be a *trans*-dihydride, {*trans*-$[CpRu(PTA)_2(H)_2]^+ \cdot (H_2O)_3$}, {**6·(H$_2$O)$_3$**}.

The *trans*-dihydride is considerably more stable than its dihydrogen tautomer (Figure 2). The transition state for the intramolecular rearrangement {**TS$_1$·(H$_2$O)$_3$**} has been located. The Gibbs energy of activation found for the conversion equals 30.3 kcal/mol, thus resulting in a quite unfavorable process. The largest change during the interconversion is undergone by the H−Ru−H angle: from 28° in the dihydrogen complex to 127° in the dihydride, its value being 103° in the transition state. The transition state has a dihydride nature. The H−H bond appears totally broken (distance H···H = 2.490 Å), whereas the two Ru−H bonds are already formed (1.590 Å). This transition state is very similar to that recently reported for the dihydrogen to dihydride isomerization in $[Cp^*FeH_2(dppe)]^+$ [dppe = 1,2-bis(diphenylphosphino)ethane].[23] The passage from the dihydrogen to the dihydride isomerization also entails the rupture of the Ru−H···O$_w$ hydrogen bond. Neither in {**TS$_1$·(H$_2$O)$_3$**} nor {**6·(H$_2$O)$_3$**} is the hydride interacting with the water molecules. On this basis, the influence of the water molecules in the homolytic splitting is minor. Without the inclusion of the three explicit water molecules a $\Delta G^{\ddagger}$ of 28.6 kcal/mol has been calculated in water.

As an alternative to the homolytic cleavage process, heterolytic H−H splitting involving a direct water effect was modeled. Using this model, the three water molecules can effectively bridge between the coordinated dihydrogen/hydride ligand and a nitrogen atom of one of the PTA ligands. The "communication" between the acidic/basic H atom and the basic N atom is henceforth achieved through an intramolecular chain of hydrogen bonds within the $Ru^{\delta+}-(H^{\delta-}-H^{\delta+})\cdots\ ^{\delta-}O(H)H^{\delta+}\cdots\ ^{\delta-}O(H)H^{\delta+}\cdots\ ^{\delta-}O(H)H^{\delta+}\cdots\ ^{\delta-}N(PTA)$ framework. Again, {**5·(H$_2$O)$_3$**} was taken as the starting point, and a first H_2 deprotonation was analyzed. *A proton transfer through the water chain* between the coordinated H_2 and one N atom of PTA takes place, with concomitant formation of {**3·(H$_2$O)$_3$**} (Figure 3). The product resulting from the process is the monohydride $[CpRu(PTA)\{PTA(H)\}H]^+$ (**3**), which has been proposed to be the active catalytic species in the biphasic hydrogenation of benzylidene acetone using $[CpRu(PTA)_2H]$.[8]

The optimized structures of the transition state for the H_2 to N proton transfer {**TS$_2$·(H$_2$O)$_3$**} and {**3·(H$_2$O)$_3$**} are shown in Figure 3. In the transition state all the O−H distances involved

(21) (a) Roger, C.; Hamon, P.; Toupet, L.; Rabaâ, H.; Saillard, J.-Y.; Hamon, J.-R.; Lapinte, C. *Organometallics* **1991**, *10*, 1045. (b) Hamon, J. R.; Hamon, P.; Toupet, L.; Costuas, K.; Saillard, J. Y. *C. R. Chim.* **2002**, *5*, 89.

(22) (a) Chinn, M. S.; Heinekey, D. M. *J. Am. Chem. Soc.* **1990**, *112*, 5166. (b) Jia, G.; Lough, A. J.; Morris, R. H. *Organometallics* **1992**, *11*, 161.

(23) Baya, M.; Maresca, O.; Poli, R.; Coppel, Y.; Maseras, F.; Lledós, A.; Belkova, N. V.; Dub, P. A.; Epstein, L. M.; Shubina, E. S. *Inorg. Chem.* **2006**, *45*, 10248.

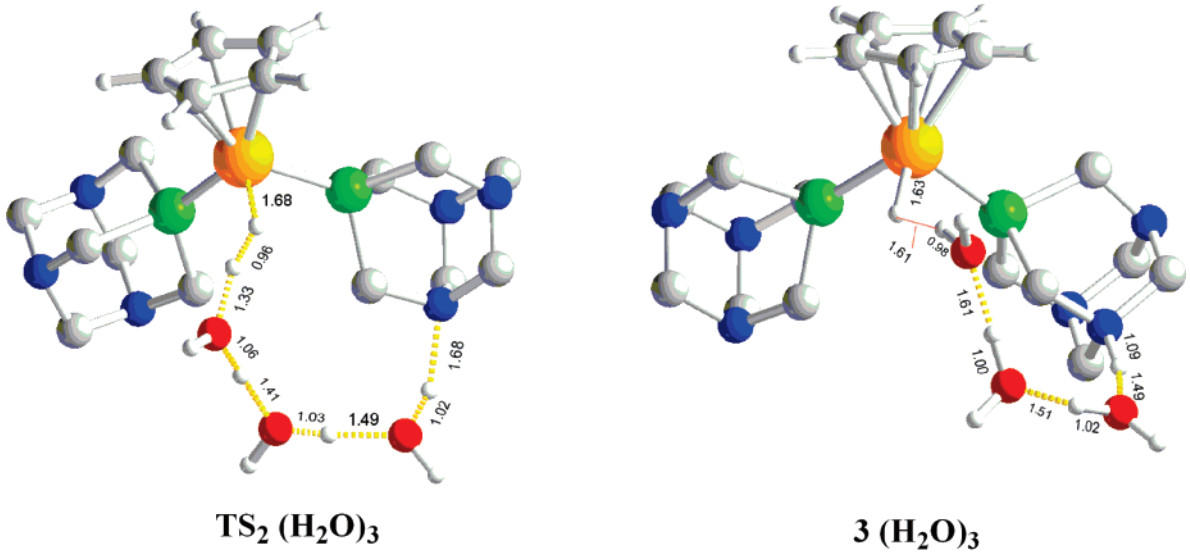

Figure 3. Optimized structures of the transition state for the heterolytic splitting {**TS$_2$·(H$_2$O)$_3$**} and the monohydride-PTA protonated product {**3·(H$_2$O)$_3$**}. Refer to the caption in Figure 1 for atom colors. Hydrogen atoms on the PTA ligands are omitted for clarity. Selected bond lengths are reported in angstroms.

in the solvent chain are intermediate between a covalent O−H bond (around 1 Å) and a true hydrogen bond (around 1.5 Å), proving the simultaneous transfer. As a result of this picture, the three solvent molecules behave as an efficient "proton carrier" to assist the intramolecular process eventually resulting in the heterolytic splitting of the molecular hydrogen ligand.

The reaction has a very low Gibbs activation energy (1.1 kcal/mol), and the final product is also exceedingly more stable than the starting solvate. {**3·(H$_2$O)$_3$**} lies 13.6 kcal/mol below the solvated dihydrogen complex {**5·(H$_2$O)$_3$**} and 5.0 kcal/mol below the dihydride {**6·(H$_2$O)$_3$**}. Both these factors favor the conversion. A similar heterolytic H_2 activation with assistance by basic N centers in the ligands was already proposed by Jalón et al. to be at work in ruthenium complexes with PPh_2py (py = pyridyl) ligands. In this case, given the proximity of the basic centers, no solvent intervention was however found to be necessary.[24] In our system, the real base that interacts with H_2 is PTA itself, which promotes the heterolytic activation of the Ru(η^2-H_2) ligand through one of its nitrogen atoms via a *solvent-mediated intramolecular proton transfer*. The mechanism can be described as a water-assisted reaction in which the water molecules act as bifunctional catalyst. Many theoretical works have already reported this kind of active participation of water chains in tautomerization[25] and proton exchange processes.[26] Our work demonstrates that this mechanism can be also operative in the heterolytic splitting of a dihydrogen ligand in water.

3. Water-Assisted Metal Protonation from [CpRu(PTA)-{PTA(H)}H]$^+$. Since the oxidative addition pathway to form the *trans*-dihydride was discarded, owing to the high activation barrier found, another option to obtain the dihydride complex {**6·(H$_2$O)$_3$**} was considered, namely, the solvent-mediated proton transfer from [*N*-PTA(H)]$^+$ to the metal. In order to allow for a further proton transfer from the [*N*-PTA(H)]$^+$ ligand to the ruthenium center, a rotation of 180° around the Ru−P bond of the protonated ligand formed in the heterolytic H−H breaking step is necessary to achieve a *transoid* conformation of the two hydrogen atoms. We have optimized the monohydride-protonated PTA in a *transoid* conformation of the N−H bond with respect to the Ru−H one (Figure 4). The *transoid* conformer {**3′·(H$_2$O)$_3$**} is slightly less stable than the *cisoid* one {**3·(H$_2$O)$_3$**}, the Gibbs energy difference in water being 3.6 kcal/mol. In {**3′·(H$_2$O)$_3$**} a water chain is also connecting two basic centers of the molecule, but a water proton points toward the metal instead of pointing toward the hydride as in **3**. The Ru···H$_w$ distance (2.590 Å) agrees with the presence of a Ru···HOH hydrogen bond.[27] The importance of Ru··HX interactionsin stabilizing the aminocyclopentadienyl ruthenium complexes has been recently recognized.[28]

Giving the large number of water molecules present in the medium, it can be assured that the arrangement found in {**3′·(H$_2$O)$_3$**} would be obtained by rotating the Ru−P bond *without moving all of the water chain*. We have estimated the energy barrier associated with the rotation of the protonated ligand, both without and with the presence of the three water molecules, by computing a potential energy curve with respect to the dihedral angle $\theta_{[H-Ru-P-C(PTA)]}$. Without the three water molecules a maximum at θ = 86.8° (intermediate value between 19.4°, initial value in {**3·(H$_2$O)$_3$**}, and 135.2°, final value in {**3′·(H$_2$O)$_3$**}) is found lying only 1.2 kcal/mol above **3**. When the three water molecules are included, the estimated barrier increases to 5.1 kcal/mol [at the same (fixed) θ value]. The barrier found is still rather low, suggesting facile ligand rotation, not hindered by the surrounding water molecules. Even if the real TS could not be located due to the limited number of water molecules considered, the rotation of the protonated ligand (PTAH)$^+$ would *not* be the rate-determining step of the overall process.

(24) Jalón, F. A.; Manzano, B. R.; Caballero, A.; Carrión, M. C.; Santos, L.; Espino, G.; Moreno, M. *J. Am. Chem. Soc.* **2005**, *127*, 15364.

(25) (a) Lledós, A.; Bertrán, J. *Tetrahedron Lett.* **1981**, *22*, 775. (b)-Ventura, O. N.; Lledós, A.; Bonaccorsi, R.; Bertran, J.; Tomasi, J. *Theor. Chim. Acta* **1987**, *72*, 175. (c) Lima, M. C. P.; Coutinho, K.; Canuto, S.; Rocha, W. R., *J. Phys. Chem. A* **2006**, *110*, 7253.

(26) (a) Bergquist, C.; Bridgewater, B. M.; Harlan, C. J.; Norton, J. R.; Friesner, R. A.; Parkin, G. *J. Am. Chem. Soc.* **2000**, *122*, 10581. (b) Prabhakar, R.; Blomberg, M. R. A.; Siegbahn, P. E. M., *Theor. Chem. Acc.* **2000**, 104, 461. (c) Jee, J.-E.; Comas-Vives, A.; Dinoi, C.; Ujaque, G.; van Eldik, R.; Lledós, A.; Poli, R. *Inorg. Chem.* **2007**, *46*, 4103.

(27) (a) Epstein, L. M.; Shubina, E. S. *Coord. Chem. Rev.* **2002**, *231*, 165. (b) Belkova, N. V.; Shubina, E. S.; Epstein, L. M. *Acc. Chem Res.* **2005**, *38*, 624.

(28) Shi, F. *Organometallics* **2006**, *25*, 4034.

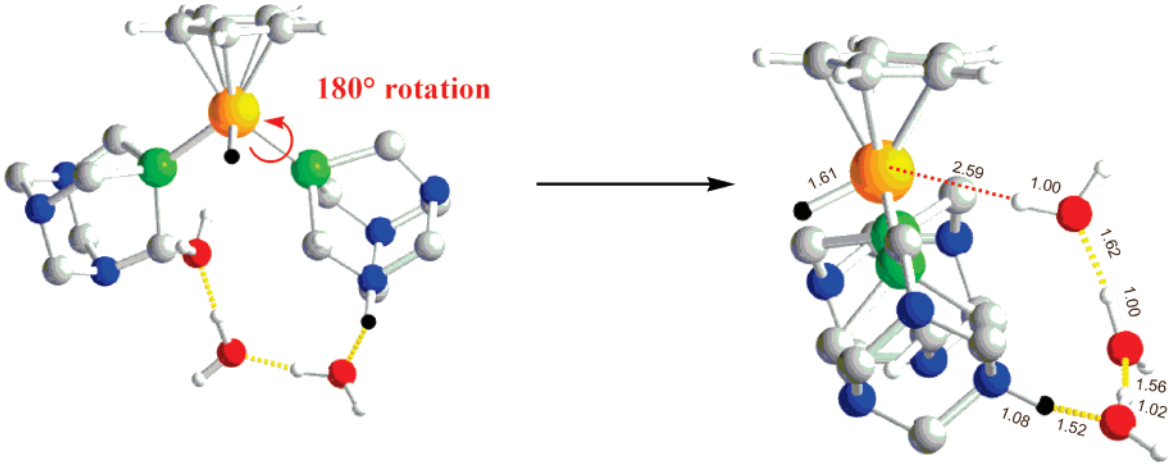

Figure 4. Rotation around the Ru−P bond of the [*N*-PTA(H)]$^+$ ligand in complex {**3·(H$_2$O)$_3$**} to get the rotamer {**3′·(H$_2$O)$_3$**}. The two hydrogen atoms in black are in a *transoid* conformation after the rotation, and the water chain is now bridging [*N*-PTA(H)]$^+$ with the Ru center. Hydrogen atoms on the PTA ligands are omitted for clarity. Selected bond lengths (Å) are reported for {**3′·(H$_2$O)$_3$**} (those of {**3·(H$_2$O)$_3$**} can be read in Figure 3).

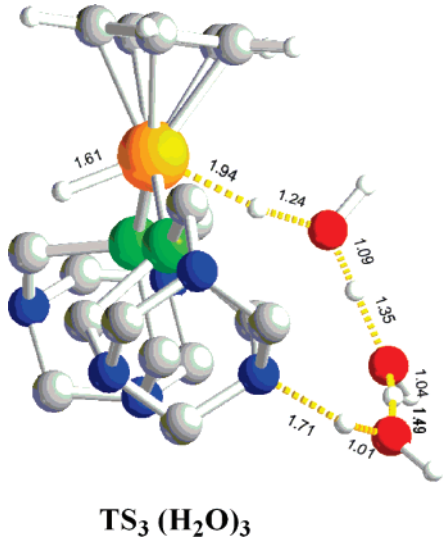

Figure 5. Transition state {**TS$_3$·(H$_2$O)$_3$**} for the metal protonation from [CpRu(PTA){PTA(H)}H]$^+$. Refer to the caption in Figure 1 for atom colors. Selected bond lengths are reported in angstroms. Hydrogen atoms on the PTA ligands are omitted for clarity.

Starting from {**3′·(H$_2$O)$_3$**} we studied the protonation at the metal center via the water chain, leading to the final *trans*-dihydride {[CpRu(PTA)$_2$(H)$_2$]$^+$·(H$_2$O)$_3$}, {**6·(H$_2$O)$_3$**}. In this reaction a proton is transferred from the {PTA(H)}$^+$ ligand to the metal. The transition state connecting the two minima {**TS$_3$·(H$_2$O)$_3$**} was located and is depicted in Figure 5. The mechanism for the metal protonation is similar to that of the hydride protonation via {**TS$_2$·(H$_2$O)$_3$**}. The Gibbs energy of activation in water was calculated at 9.1 kcal/mol, and the reaction was found to be endoergonic by 1.4 kcal/mol (Figure 6). The barrier for the protonation of the metal is considerably higher than for the protonation of the *N*-PTA. The same result has been found for the protonation of [Cp*Fe(dppe)H] with acids.[29]

4. Overall Process. In Figure 6, a Gibbs energy scheme for the overall process of heterolytic H−H bond splitting in water is shown. The interaction of H_2 with [CpRu(PTA)$_2$]$^+$ affords three minima: an initial dihydrogen complex **5** and two products resulting from the H−H breaking: the monohydride-PTA protonated complex **3** and the classical dihydride **6**. These three complexes have also been invoked in the protonation equilibria resulting from the protonation of [CpRu(PTA)$_2$H] with HBF_4.[8b]

[CpRu(PTA){PTA(H)}H]$^+$ appears to be the deeper minimum. The dihydride **6** is also considerably more stable than the dihydrogen initial complex **5**. The first step implying the heterolytic breakage of the coordinated H_2 is much easier than the second one involving protonation of the metal. It is clear from the ΔG profile that the dihydrogen complex is a rather unstable intermediate that evolves quickly toward [CpRu(PTA)-{PTA(H)}H]$^+$. The highest Gibbs energy difference is around 12.7 kcal/mol, corresponding to the ΔG between {**3·(H$_2$O)$_3$**} and {**TS$_3$·(H$_2$O)$_3$**}. It is reasonable to think that the stable intermediate species {**3·(H$_2$O)$_3$**} is not likely to evolve to the dihydride {**6·(H$_2$O)$_3$**}, in accordance with the experimental results, where neither the classical dihydride nor the dihydrogen complex were detected as a result of the interaction of **1** with H_2.

The values depicted in the profiles of Figures 2 and 6 are Gibbs energies in water (ΔG_{water}) obtained adding to the Gibbs energies in the gas phase the contribution to the Gibbs energy of solvation measured by the continuum model. Thus the computed entropic contributions refer to gas phase and neglect solvation and desolvation effects in solution. How the entropic effects in solution can be taken into account in calculations is a subject under current discussion.[30] In order to assess the importance of entropic effects in the mechanism, we report in Figure 7 a comparison between the ΔG and ΔE profiles in water, ΔE_{water} resulting from adding the contribution of the Gibbs energy of solvation to the gas-phase internal energies. As it can be seen, the profiles are very similar, thus indicating that entropic effects are of minor importance and that *the enthalpic factor is predominant in determining the final Gibbs energy values*. The largest difference is found in the slight entropic destabilization of species {**3·(H$_2$O)$_3$**} and {**3′·(H$_2$O)$_3$**}. The small entropic effect found can be explained by the absence of steps implying

(29) Belkova, N. V.; Collange, E.; Dub, P.; Epstein, L. M.; Lemenovskii, D. A.; Lledós, A.; Maresca, O.; Maseras, F.; Poli, R.; Revin, P. O.; Shubina, E. S.; Vorontsov, E. V. *Chem.−Eur. J.* **2005**, *11*, 873.

(30) (a) Braga, A. A. C.; Ujaque, G.; Maseras, F. *Organometallics* **2006**, *25*, 3647. (b) Tuttle, T.; Wang, D.; Thiel, W.; Köhler, J.; Hofmann, M.; Weis, J. *Organometallics* **2006**, *25*, 4504.

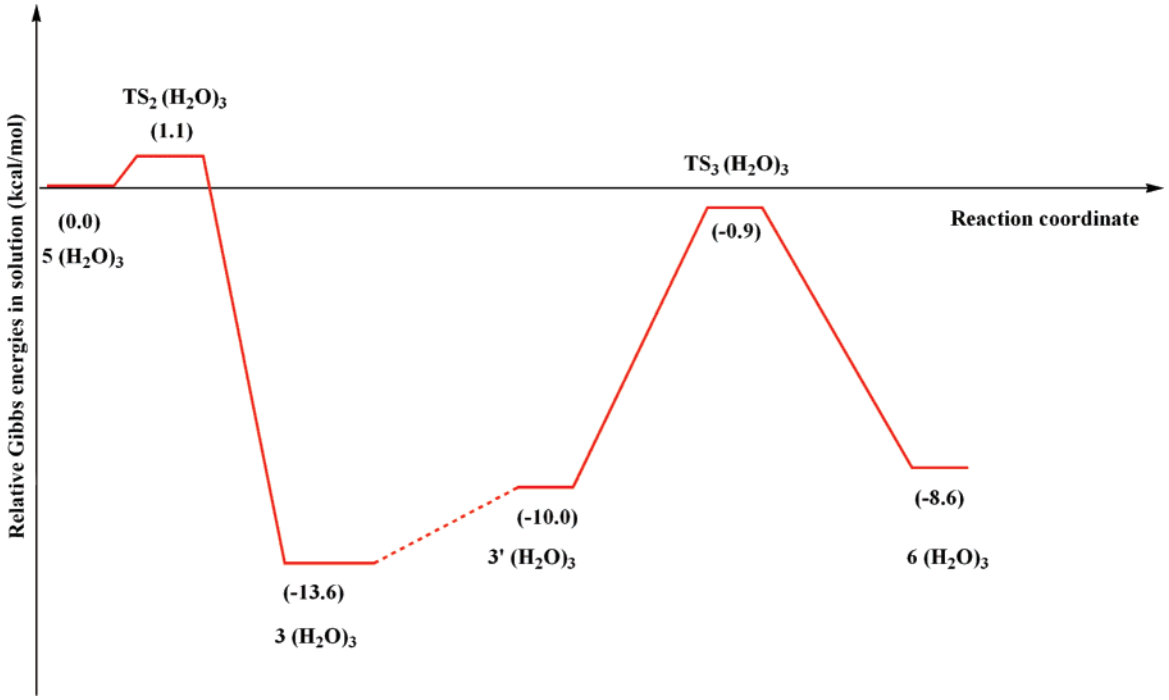

Figure 6. Overall Gibbs energy profile for the H_2 heterolytic splitting in water.

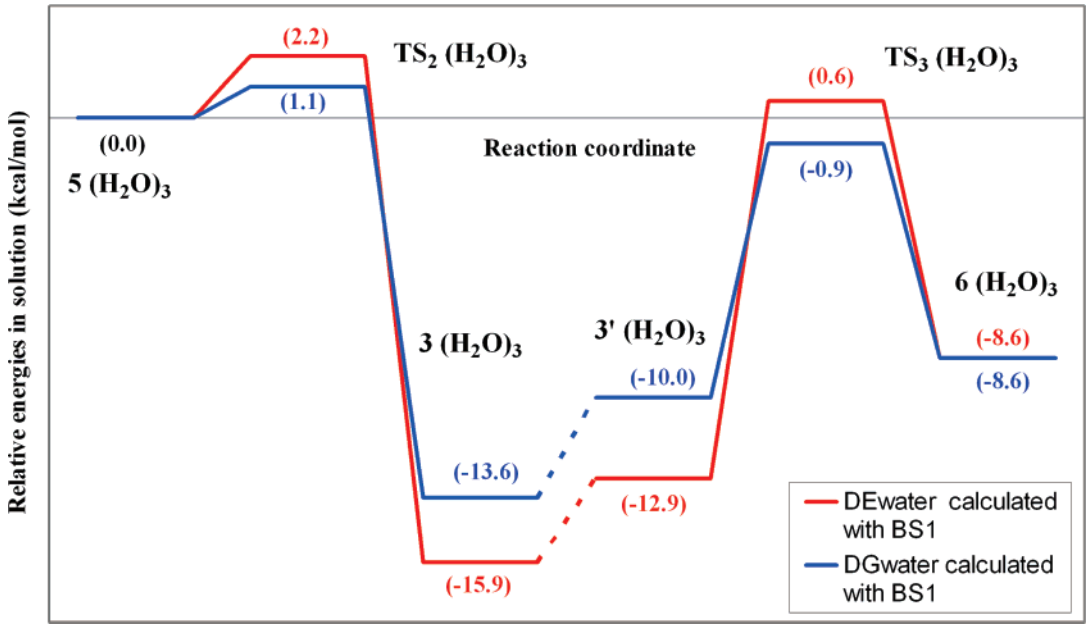

Figure 7. Comparison between ΔG_{water} (blue line) and ΔE_{water} (red line) for the profile of the H_2 heterolytic splitting (see also Figure 6).

ligand association or dissociation in the overall mechanism. In addition, it has to be underlined that in water solution an *ordered* disposition (like chains or clusters) of the solvent molecules *already exists* even without the solute, this decreasing the entropic penalty related to the formation of water chains in our mechanism.

The last point to be discussed is the basis set dependence on the results. An extended hydrogen-bonded network involving three water molecules of the computational model and the basic centers of the complexes is present in all the optimized structures found; its energy can be affected by the enlargement of the basis set. To assess the basis set effect, the internal energies of all the optimized species have been recalculated using a larger basis set (BS2). The comparison between the ΔE_{water} profiles obtained with both sets is shown in Figure 8. The basis set extension affects the energy profile significantly. With BS2 the relative energies of transition states and hydride intermediates increase with respect to that of the dihydrogen complex, as can be seen comparing the red and the yellow profiles in Figure 8. The first transition state rises from 2.2 kcal/mol above **5** (BS1) to 9.3 kcal/mol (BS2). Intermediates **3**, **3′**, and in part **6** are also notably destabilized with respect to **5** when enlarging the basis set. As a consequence, the energy barrier for the first step rises considerably, whereas the increase of the energy barrier for the metal protonation is smaller.

However, the main conclusions we inferred from calculations with BS1 are still valid with BS2: the monohydride-PTA protonated complex **3** is the most stable species and its formation

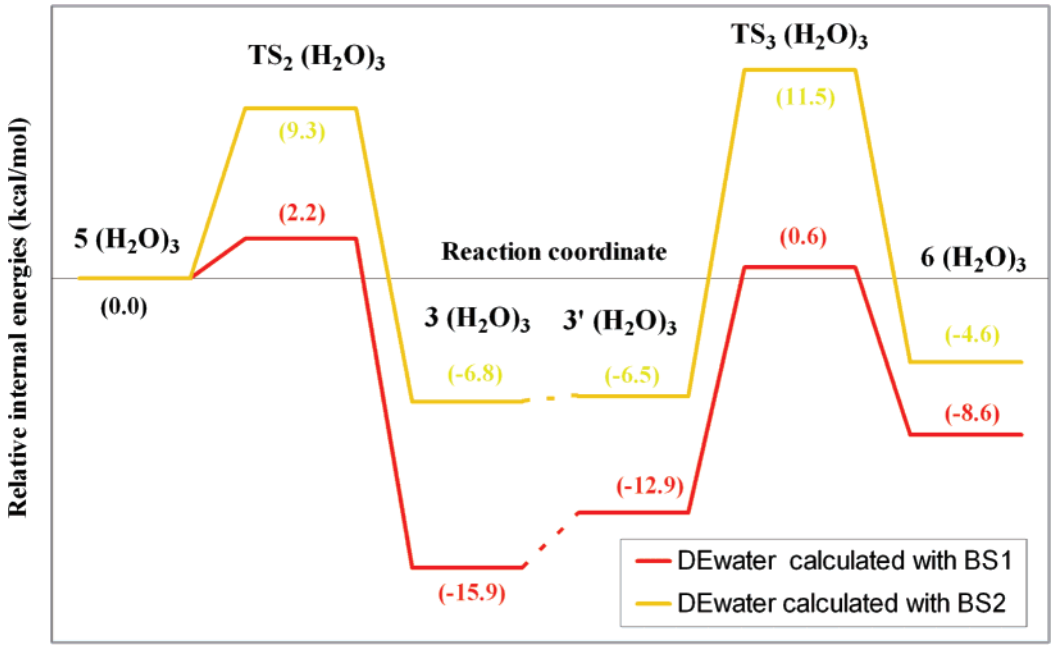

Figure 8. Comparison between ΔE_{water} for the overall profile for the H_2 heterolytic splitting obtained with basis set 1 (BS1) and basis set 2 (BS2). See also Figure 6.

by heterolytic splitting of the H_2 ligand in **5** has a lower barrier than its further evolution toward **6**.

Concluding Remarks

In conclusion, the present DFT study on the role of water in the activation of dihydrogen by **1** has revealed that water takes an active part in assisting the heterolytic splitting of the H−H bond. The ability of water to form extensive hydrogen bonding is essential to lower the energy barriers, compared to other mechanisms where no direct involvement of the solvent is postulated. In addition, our calculations show that a ruthenium-coordinated PTA ligand efficiently assists the heterolytic splitting by taking up a proton from H_2 via N-quaternization and confirm, in line with experimental results, that the formation of a monohydrido species is favored over the *trans*-dihydride. Additional calculations are in progress to extend this study to [Cp*Ru(PTA)$_2$Cl] (Cp* = C_5Me_5), as the more basic properties of the permethylated ring may significantly modify the reactivity of the system in assisting hydrogen splitting.

Acknowledgment. We thank ECRF through project Firenze Hydrolab for sponsoring a postdoctoral grant to A.R., and EC for funding through Aquachem and Hydrochem projects (MRTN-CT-2003-503864 and HPRN-CT-2002-00176). A.L. acknowledges support from the Spanish MEC (project CTQ2005-09000-C02-01).

Supporting Information Available: Optimized geometries (Cartesian coordinates) and gas-phase potential and Gibbs energies as well as Gibbs energies in water of the calculated species. This material is available free of charge via the Internet at http://pubs.acs.org.

OM061023A